dicating that the intrinsic losses as well as the mode conversion levels are indeed very low.

Although these filters have been designed as low-pass filters, the close agreement between measurement and analysis strengthens our belief that their application should not be limited in this way. We envision possible applications as broad-band bandpass as well as bandstop filters, in the millimeter wave region as well as in other frequency ranges.

ACKNOWLEDGMENT

The authors wish to thank many of their colleagues at the Bell Laboratories, whose cooperation has made the progress of this project possible. Especially, they would like to thank R. P. Hecken, H. A. Kvinlaug, and J. C. Williams for their efforts in the computer-aided design and physical realization studies during the early phase of this program.

REFERENCES

[1] G. L. Matthaei, L. Young, and E. M. T. Jones, *Microwave Filters, Impedance-Matching Networks and Coupling Structures.* New York: McGraw-Hill, 1964.
[2] P. T. Hutchinson, "A digital millimeter wave waveguide transmission system," in *Trunk Telecommunication by Guided Waves Conference Dig., Publ. No. 71*, 1970, pp. 159–164.
[3] E. A. Marcatili and D. L. Bisbee, "Band splitting filters," *Bell Syst. Tech. J.*, vol. 40, pp. 197–213, Jan. 1961.
[4] L. Young and E. G. Cristal, "Low-pass and high-pass filters consisting of multilayer dielectric stacks," *IEEE Trans. Microwave Theory Tech.*, vol. MTT-14, pp. 75–80, Feb. 1966.
[5] L. B. Felsen and N. Marcuvitz, *Radiation and Scattering of Waves.* Englewood Cliffs, N. J.: Prentice-Hall, 1973.
[6] R. Levy, "A generalized design technique for practical distributed reciprocal ladder networks," *IEEE Trans. Microwave Theory Tech.*, vol. MTT-21, pp. 519–526, Aug. 1973.
[7] W. A. Davis and P. J. Khan, "Coaxial bandpass filter design," *IEEE Trans. Microwave Theory Tech.*, vol. MTT-19, pp. 373–380, Apr. 1971.
[8] R. Levy, "Tables of element values for the distributed low-pass prototype filter," *IEEE Trans. Microwave Theory Tech. (Special Issue on Microwave Filters)*, vol. MTT-13, pp. 514–536, Sept. 1965.
[9] *Dielectric Materials and Applications*, A. R. Von Hippel, Ed. Cambridge, Mass.: M.I.T. Press, 1954.

Integrated Fin-Line Millimeter Components

PAUL J. MEIER, SENIOR MEMBER, IEEE

***Abstract*—This paper reviews the characteristics of integrated fin-line, a low-loss transmission line which is compatible with batch-processing techniques and superior to microstrip in several respects at millimeter wavelengths. Relative to microstrip, fin-line can provide less stringent tolerances, greater freedom from radiation and higher mode propagation, better compatibility with hybrid devices, and simpler interfaces with waveguide instrumentation. Examples of solid-state and passive components are presented which illustrate the potential of integrated fin-line at millimeter wavelengths. The examples include a p-i-n attenuator which has demonstrated the capability of constructing low-loss semiconductor mounts in fin-line. A four-pole bandpass filter, which performs in close agreement with theory, is also discussed.**

INTRODUCTION

INCREASED activity in the spectrum above 30 GHz has recently stirred interest in the development of millimeter integrated circuits. Much of the enthusiasm associated with integrated circuits can be traced to the clear advantages that such circuits provide below 3 GHz, namely, reduced size, weight, and cost combined with improved electrical performance, production uniformity, and reliability. However, those who have worked with integrated circuits at centimeter wavelengths (3–30 GHz) have encountered some fundamental problems which have limited the utility of such circuits. These problems include the critical tolerances and questionable production uniformity that can occur when miniaturization is carried too far. Although enhanced performance is possible in centimeter integrated circuits through the reduction of parasitics and the elimination of superfluous interfaces, poorer overall performance is also possible. The fundamental microstrip problems, which generally increase in severity as the operating frequency is raised, include radiation loss, spurious coupling, dispersion, and higher mode propagation. Attempts to integrate a large number of components in a single housing have generally demonstrated the need for "mode barriers" and "box-resonance absorbers." Radiation and related problems can be controlled by choosing progressively thinner substrates as the operating frequency is raised, but this only serves to degrade the Q factor, compound tolerance problems, and restrict the range over which the characteristic impedance can be varied.

Although standard microstrip techniques can be applied to millimeter components [1], [2], the problems listed

Manuscript received May 8, 1974; revised August 30, 1974.
The author is with AIL, a Division of Cutler-Hammer, Melville, N. Y. 11746.

previously can be expected to become more severe. As the operating frequency is raised and the microstrip dimensions are decreased, a limit will be reached where the strip width is no longer compatible with chip and beam-lead devices. In addition, millimeter integrated circuits must be tailored to requirements that are generally different from those which apply at lower frequencies. For example, the ability to construct a simple transition to waveguide becomes important at millimeter wavelengths where coaxial instrumentation is not practical. Moreover, the miniaturization that proved to be an asset at centimeter wavelengths can become a liability in millimeter applications. Designers of millimeter equipment have historically selected quasi-optical approaches to *increase* the physical size of components and thereby ease tolerance problems and improve performance [3]. Thus the ideal transmission line for millimeter integrated circuits is one which avoids miniaturization and yet offers the potential for low-cost production through batch-processing techniques. Integrated fin-line [4]–[6] is such a transmission line.

After introducing the symbols to be utilized throughout this paper, the body of the text will review the characteristics of integrated fin-line and demonstrate how this transmission line can be profitably applied to solid-state and passive millimeter components. Conclusions will then be presented regarding the potential application of integrated fin-line to future millimeter systems.

NOMENCLATURE

a	Major inner dimension of fin-line housing.
b	Minor inner dimension of fin-line housing.
c	Thickness of dielectric substrate.
d	Gap between fins.
s	Equivalent ridge thickness.
B	Susceptance magnitude.
k_e	Equivalent dielectric constant.
Q	Unloaded quality factor.
Y_0	Characteristic admittance of fin-line.
Z_0	Characteristic impedance of fin-line $= 1/Y_0$.
R_0	Resistance of load matched to Z_0.
Z_∞	Characteristic impedance at infinite frequency.
λ_g	Guide wavelength.
λ_0	Free-space wavelength.
λ_c	Cutoff wavelength of equivalent ridged waveguide.
C_j, R_j	Capacitance and resistance of p-i-n junction.
L_s, R_s	Series parasitic inductance and resistance of p-i-n diode.
C_p	Capacitance of diode package.
L_{s1}	Series inductance external to diode package.
W	Width of inductive strip.

CHARACTERISTICS OF INTEGRATED FIN-LINE

In an integrated fin-line structure [4], metal fins are printed on a dielectric substrate which bridges the broad walls of a rectangular waveguide. This adaptation of ridge-loaded waveguide permits circuit elements to be photoetched by low-cost batch techniques. The dimensions of practical fin-line circuits remain compatible with chip and beam-lead devices throughout the millimeter spectrum, thereby offering great potential for the construction of active and passive hybrid integrated circuits. Examples of such circuits and a simple low-reflection transition to rectangular waveguide will be presented.

In addition to serving as the bonding areas for hybrid devices, the printed fins increase the separation between the first two modes of propagation thereby providing a wider useful bandwidth than conventional waveguide. Owing to the similarity between integrated fin-line and conventional ridged waveguide, considerable design information [7], [8] is available. For thin substrates of moderate permittivity, the dielectric will have a minor effect [9] and single-mode bandwidth and attenuation of integrated fin-line may be estimated from existing data [8]–[10]. Such estimates lead to the conclusion that integrated fin-line can provide bandwidths in excess of an octave with less attenuation than microstrip. Larger single-mode bandwidths are feasible at the expense of attenuation.

The low-loss properties of integrated fin-line have been experimentally demonstrated through cavity tests at centimeter wavelengths [5] and transmission tests at millimeter wavelengths [11]. Preliminary tests were conducted at X band where wide-band sweepers were more readily available. The substrate thickness, however, was chosen to be sufficiently large (0.062 in) to permit direct scaling to higher frequencies.

Two different fin-line configurations, as shown in Fig. 1, were evaluated. In the configuration of Fig. 1(a), the fins are printed on opposite sides of a single dielectric substrate. Since the fins are directly grounded to the metal waveguide walls, this configuration is applicable only to passive devices. In the configuration of Fig. 1(b), however, the fins are printed on the mating surfaces of two dielectric substrates. Since the fins are insulated from the waveguide at dc, bias may be introduced for active components. RF continuity between the fins and the waveguide wall is obtained by choosing the thickness of the broad walls to be a quarter wavelength in the dielectric medium and by selecting $c \ll a$. The resultant choke prevents radiation or TEM propagation across a bandwidth in excess of an octave.

Teflon-fiber glass (3M type FL-GT) substrates with normalized gaps ranging from $d/b = 0.1$ to 1.0 were evaluated in the cavity whose aspect ratio (b/a) was 0.45. The center frequency and 3-dB bandwidth were recorded for each sample and the results were analyzed to determine the manner in which the guide wavelength and unloaded Q varied.

Fig. 2 shows how the measured Q (including the effect of losses within the irises) varies with respect to the gap between the fins. For moderate loading $(d/b \geq 0.6)$, the measured Q of integrated fin-line exceeds 400 for insulated fins, and is better than 700 for the grounded-fin configura-

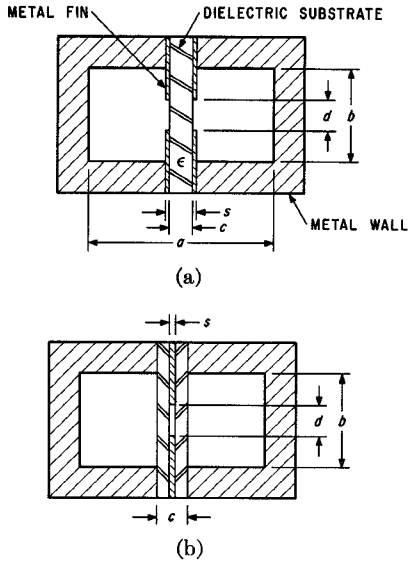

Fig. 1. Fin-line cavity configurations. (a) Grounded fins. (b) Insulated fins.

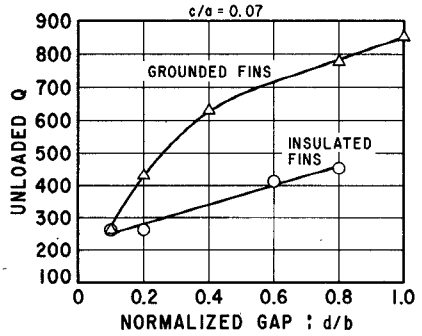

Fig. 2. Measured Q of integrated fin-line.

tion. These values compare favorably with those reported for practical microstrip lines at centimeter wavelengths [12].

To supplement the earlier measurements of unloaded Q performed in the 3-cm band, the insertion loss of integrated fin-line has been measured for a comparable fin-line structure in the 9-mm band [11]. A copper-clad laminate (Duroid 5880) with a thickness of 0.020 in was selected to maintain the ratio of c/a at 0.07. By accurately measuring the insertion loss of two fin-line transmission fixtures of different lengths, the loss was found to be 0.1 dB/wavelength for grounded fins with $d/b = 0.1$. This corresponds to an unloaded Q of 273, which is in agreement with the X-band cavity measurement of 260. Since the latter figure is somewhat pessimistic owing to loss in the coupling irises, it may be concluded that the loss in integrated fin-line holds fairly constant throughout the frequency range of 10–40 GHz. Although the loss can be expected to increase gradually as the frequency is raised above 40 GHz, the general utility of fin-line should be preserved throughout the millimeter spectrum.

Another important property of integrated fin-line is the guide-wavelength variation which can be calculated from the simple equation

$$\lambda_g = \frac{\lambda_0}{[k_e - (\lambda_0/\lambda_c)^2]^{1/2}} \quad (1)$$

where k_e is the equivalent dielectric constant, λ_0 is the free-space wavelength, and λ_c is the cutoff wavelength for an air-filled ridge-loaded waveguide of the same dimensions [8]. The value of k_e may be experimentally determined for a given fin-line configuration from a single cavity test [5]. It has been shown that the value of k_e varies little with respect to d/b when the fins are grounded directly to the waveguide. When d/b approaches unity, the value of k_e determined from the cavity agrees with the published value [10] for both the grounded and insulated cases. As the gap between the insulated fins becomes smaller, however, the value of k_e approaches the dielectric constant of the substrate material. Representative values of k_e appear in Table I.

To confirm the validity of (1) and demonstrate the capability of integrated fin-line at millimeter wavelengths, a transmission fixture was developed for operation in the frequency range of 26.5–40.0 GHz. Fig. 3 shows the cross section of this structure which is suitable for mounting semiconductor devices. In this structure, the upper fin is insulated from the housing at dc by a dielectric gasket, but is grounded at RF by choosing the thickness of the broad walls to be a quarter wavelength in the dielectric medium. The lower fin is grounded directly by a metal gasket to provide a dc return in solid-state applications. Nylon screws hold the halves of the housing together and align the substrate and its associated gaskets. Nylon is preferable to metal as the former has little effect on the RF choke formed within the broad walls.

The guide wavelength in the millimeter fin-line fixture has been measured across the band of 26.5–40.0 GHz by a sliding short-circuit technique. The fin-line was connected to a conventional slotted line through a low-reflection transition and the fin-line was internally terminated in a sliding short circuit of special design. The short consisted of a forked structure which straddled the dielectric substrate and provided a high standing wave ratio (SWR) by means of noncontacting chokes. The measurement was performed by recording the distance through which the short was moved in order to repeat nulls observed at a fixed location in the slotted line. Fig. 4 is a plot of the measured guide wavelength as a function of frequency for a typical structure ($d/b = 0.13$) suitable for mounting semiconductor devices. The value of k_e was determined by substituting into (1) the measured λ_g at 31 GHz ($\lambda_0 = 0.3807$ in) and the published value of λ_c [8] for an air-filled ridged waveguide of the same dimensions ($s/a \approx 0$, $a = 0.280$ in). Based upon this single-frequency measurement, the value of k_e was determined to be 1.31. Also shown in Fig. 4 is the curve calculated by applying (1) throughout the band for $k_e = 1.31$. The measured values of λ_g agree with the calculation ± 2 percent across the 40-percent instrumentation band.

To predict the behavior of semiconductor devices in fin-line, it is helpful to know the absolute value of the

TABLE I

EQUIVALENT DIELECTRIC CONSTANT

Dielectric Constant of Substrate Material	Fin-Line Configuration	s/a	d/b	Equivalent Dielectric Constant k_e
2.5	Figure 1A	0.07	0.1	1.50
2.5	Figure 1A	0.07	1.0	1.25
2.5	Figure 1B	0.07	0.1	2.10
2.5	Figure 1B	0.07	1.0	1.25
2.2	Figure 3	0.036	0.08	1.33
2.2	Figure 3	0.036	0.13	1.31

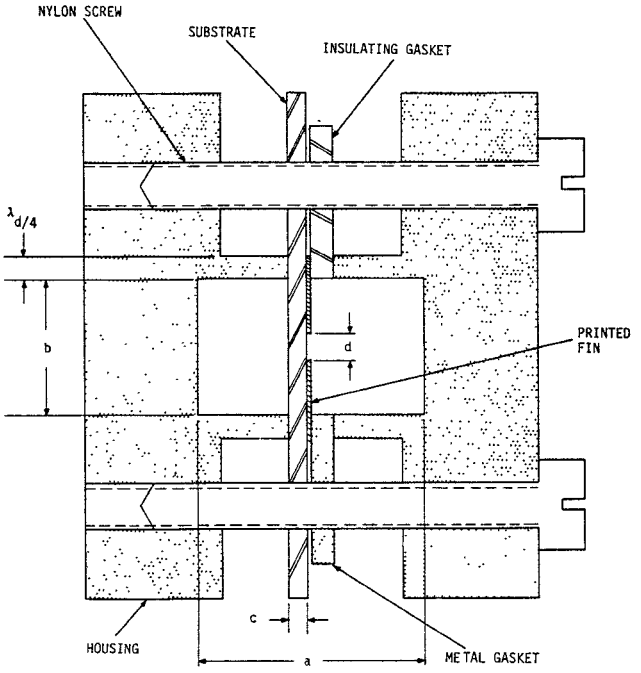

Fig. 3. Integrated fin-line semiconductor mount.

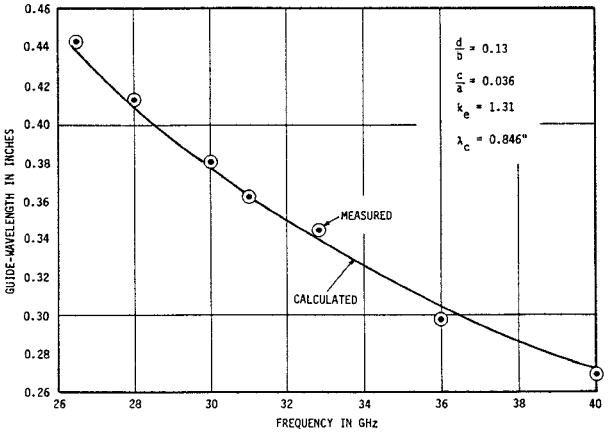

Fig. 4. Wavelength in insulated fin-line.

characteristic impedance ($Z_0 = 1/Y_0$). Values of the characteristic admittance of ridge-loaded waveguide, based upon a power-voltage definition, have been published for a wide range of parameters [8]. It has been found that these data are directly applicable to fin-line structures containing thin substrates ($c/a < 0.1$) of moderate permittivity. The characteristic impedance of fin-line may be approximated by

$$Z_0 \approx \frac{Z_\infty}{[k_e - (\lambda_0/\lambda_c)^2]^{1/2}} \tag{2}$$

where Z_∞ is the characteristic impedance of a ridge-loaded waveguide of the same dimensions at infinite frequency (that is, the reciprocal of the published admittance values). Appropriate factors may be applied to account for other aspect ratios (b/a), configurations (single versus double ridge), and impedance definitions [13].

Based upon a knowledge of the basic characteristics discussed previously, one may design a wide range of solid-state and passive components in integrated fin-line. The following sections will present examples of such components which serve to illustrate the advantages of fin-line construction techniques.

APPLICATION TO SOLID-STATE DEVICES

A millimeter demonstration of the compatibility of integrated fin-line with semiconductors has been performed with the aid of the previously discussed transmission fixture (Fig. 3). Additional features of this fixture appear in Fig. 5, wherein the fully assembled fixture is shown adjacent to a duplicate set of components. The housing mates directly with two standard WR28 waveguides and has identical inner dimensions (0.140 × 0.280 in). The substrate is cut from a 0.010-in sheet of laminate (Duroid 5880) and includes six mounting holes and two stepped edges. The latter protrude into the abutting WR28 waveguides and serve as quarter-wave transformers. After establishing a low-reflection transition between the WR28 waveguide and a slotted waveguide loaded by a dielectric slab ($d/b = 1.0$), the substrate metallization is tapered until the desired gap between the fins is obtained. The illustrated transitions at the ends of the substrate are each three wavelengths long near the middle of the instrumentation band (33 GHz). The measured VSWR of each transition is 1.2 or better across the 26.5–40-GHz band. It is believed that a more compact transition is feasible with quarter-wave transformers substituted for the fin-line taper. The substrate metallization also includes an RF blocking network connected to the upper fin.

To demonstrate the compatibility of integrated fin-line with semiconductor devices, two beam-lead p-i-n diodes (Alpha D5840B) were mounted across the fins near the center of the previously discussed substrate ($d/b = 0.13$). The diodes were spaced a quarter wavelength apart at a frequency near the upper end of the instrumentation band. The measured insertion loss of the p-i-n fin-line attenuator is plotted in Fig. 6 as a function of bias with frequency as a parameter. At the lower end of the band, where parasitics play a minor role, the reversed-bias insertion loss of the attenuator is only 0.3 dB, thereby demonstrating the capability of constructing low-loss semiconductor mounts in fin-line. As the bias is varied in the forward direction,

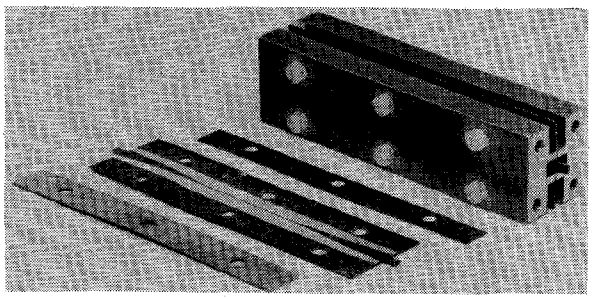

Fig. 5. Fin-line test fixture.

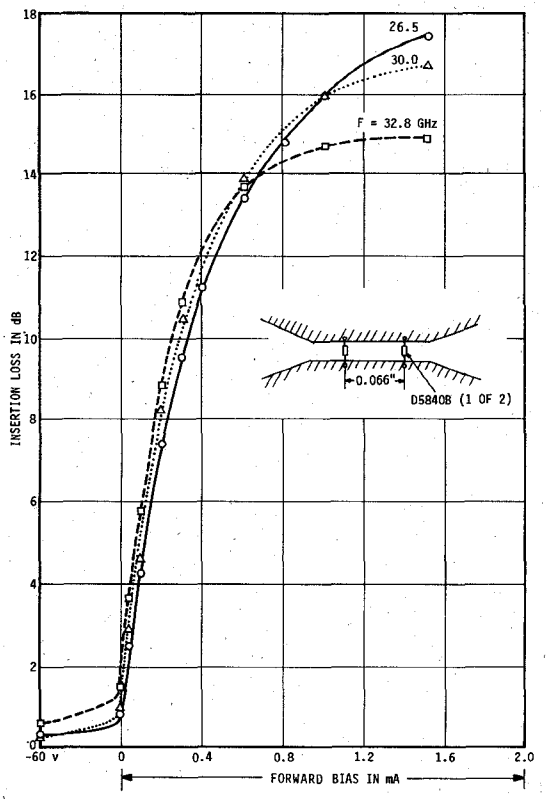

Fig. 6. Insertion loss of fin-line attenuator.

the attenuation varies smoothly over a 14-dB range throughout a 20-percent band.

Although the preliminary results of Fig. 6 are gratifying, it may be observed that the minimum loss and maximum attenuation deteriorate as the frequency is raised. To obtain a better understanding of the frequency limitations of this design, a program was launched to obtain an equivalent circuit for the attenuator, including the parasitic elements associated with the diode and its mounting structure. The SWR, as a function of bias and frequency, was measured for a single diode mounted across a matched fin-line. A computer-aided technique was then applied to find the parasitic elements which best reconciled the measured data with the general equivalent circuit shown in Fig. 7. Based upon the manufacturer's published data, a value of 1 Ω was assigned to R_s and R_j was represented as

$$R_j = 14.1I^{-0.83} \tag{3}$$

where I is the diode current in milliamperes ($0.02 \leq I \leq 2$). All other parasitics were assigned plausible initial values and then optimized by an iterative process. Based upon a power-voltage definition of Z_0, the fit between the measured and calculated values of SWR proved to be only fair after exhaustive iterations. Moreover, the optimum value of C_j was found to be well below the specified value of 0.03 pF. Consequently, other definitions of Z_0 were examined; the best overall fit was obtained by adopting the power-current definition and thereby reducing Z_∞ by a factor of $\pi^2/16$ [13].

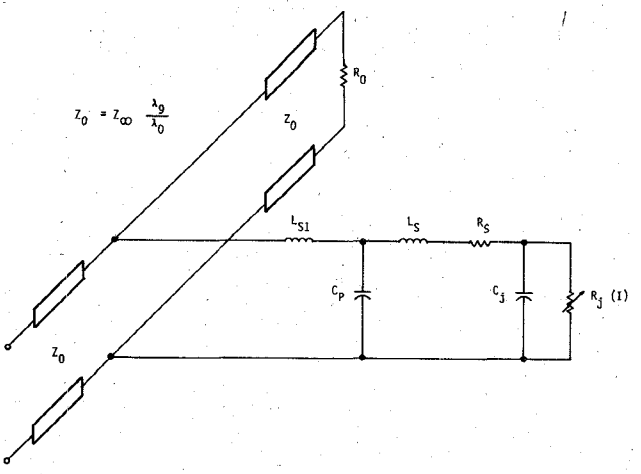

Fig. 7. Equivalent circuit for p-i-n diode.

Table II lists the values of the parasitic elements that provided the best fit (rms error equals 4 percent) with 21 SWR measurements at three equally spaced frequencies from 26.5 to 40.0 GHz and seven logarithmically spaced bias currents from 0 to 1.5 mA. This simple technique provided an unambiguous determination of the parasitics without complex impedance measurements (which prove difficult to reference at the plane of the diode). The validity of the equivalent circuit was confirmed by accurately predicting the total insertion loss of the diode which is generally greater than that due to the observed SWR alone.

The key parasitic element, which limits the high-frequency performance in the existing test fixture, is the series inductance L_s. The inductive reactance at 40 GHz is 35 Ω, which is significant relative to the forward-biased junction resistance and the characteristic impedance of the line ($Z_0 = 73.5$ Ω). This accounts for the reduced attenuation under forward bias. For reverse bias, the series inductance tends to resonate with the junction capacitance, thereby introducing a reflection which increases the minimum insertion loss.

The high-frequency response of the p-i-n attenuator may be improved by several methods. The series inductance can be lowered by decreasing the gap between the fins; however, this further reduces Z_0 and compounds the problem under forward bias. A better approach is to raise Z_0 by constricting the width of the fin-line housing and thereby increasing the ratios λ_g/λ_0 and b/a. This minimizes the effect of the series inductance under forward bias and increases the maximum attenuation. Raising Z_0 will also

TABLE II

P-I-N EQUIVALENT CIRCUIT PARAMETERS

L_s	= 0.14 nH
L_{s1}	≈ 0
C_p	= 0.002 pF
C_j	= 0.037 pF
Z_∞	= 80.6 ohms [a]

[a] Power current definition.

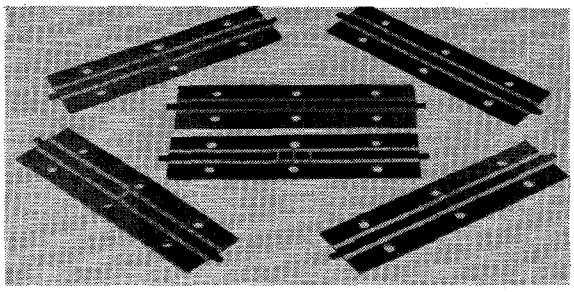

Fig. 8. Filter components.

increase the reflection of a single diode under reverse bias, but this can be offset over a moderate bandwidth by spacing two diodes such that their reflections cancel. The upper frequency limitation then becomes the series resonance between L_s and C_j which is 70 GHz for the parasitics listed in Table II. Substituting a diode with a smaller junction capacitance (such as the D5840E) can move this series resonance well above 100 GHz. Further increases in the operating frequency and bandwidth are feasible with a more complex fin-line mount which tunes out the inductance L_s.

A p-i-n attenuator has been selected for measurements and analysis to demonstrate the potential of a broad class of semiconductor fin-line components. Other solid-state millimeter components which are amenable to fin-line construction include mixers, oscillators, amplifiers, limiters, switches, and phase shifters. A fin-line Gunn oscillator, which provides a power output of 45 mW in the 9-mm band, has been described elsewhere [14]. In addition to the existing examples of one- and two-port components, fin-line is well suited to the fabrication of E-plane Y junctions. Consequently, three-port networks, such as parametric amplifiers, phase modulators, and switching matrices, are feasible. For the reasons presented previously, integrated fin-line is preferred to microstrip for the construction of solid-state components and systems throughout the millimeter spectrum.

APPLICATION TO PASSIVE COMPONENTS

Although fin-line configurations with insulated fins and small gaps are best suited to solid-state applications, lower loss can be obtained with grounded fins and larger gaps. It has been shown, in connection with the discussion of Fig. 2, that an unloaded Q of 700–850 is possible for grounded fins with moderated loading ($d/b > 0.6$). Although another planar configuration [15] will provide higher values of Q, many millimeter applications exist where fin-line should prove to be adequate.

To demonstrate the capability of fin-line components fabricated according to the cross section of Fig. 1(a), various filter components were printed on 0.020-in Duroid. Test samples include the one- and four-pole inductively coupled filters shown at the center of Fig. 8, surrounded by four substrates, each printed with a single inductive element. By measuring the insertion loss of these elements across the 26.5–40-GHz band, families of design curves were generated to present the shunt susceptance as a function of strip width, with free-space wavelength as a parameter.

Fig. 9 shows how the shunt susceptance (normalized to the characteristic admittance of the fin-line) varies with respect to the strip width (normalized with respect to the wide inner dimension of the housing) for the special case of $d/b = 1.0$. Larger values of B/Y_0 can be obtained for a given w/a by reducing d/b but only at the expense of the unloaded resonator Q. Additional one-pole resonator measurements have been performed to determine the unloaded resonator Q and the reference plane at which the inductive strip can be modeled as a pure shunt susceptance. Based upon the characterization of fin-line filter elements and published design curves [16], a four-pole equal-element filter has been constructed and tested. Fig. 10 compares the calculated response with measurements. The calculation was performed by a computer-aided technique which solves for the overall $ABCD$ matrix of the entire filter network including:

1) shunt susceptance of each filter element and its variation with respect to frequency;

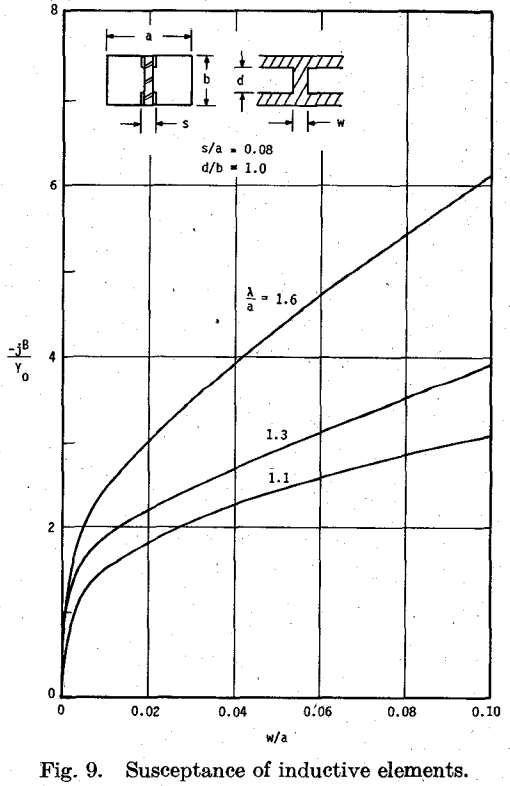

Fig. 9. Susceptance of inductive elements.

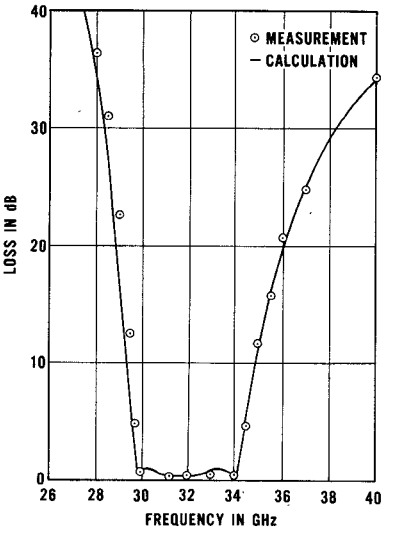

Fig. 10. Response of four-pole filter.

2) offset between the electrical and mechanical centerlines of the inductive elements;

3) variation of guide wavelength with respect to frequency, which is known accurately for $d/b = 1.0$ [5], [10].

4) unloaded resonator Q of 350 for center sections (based upon one-pole measurement).

The good agreement that has been obtained between measurements and theory serves to illustrate the straightforward application of fin-line techniques to the design of millimeter filters.

To explore the possible advantages of fin-line filters with $d \neq b$, the susceptance of a more generalized fin-line inductor has been measured. Table III lists the susceptance measured at three frequencies across the instrumentation band for two inductor configurations. For the first configuration, the fins do not load the waveguide and a fairly wide strip ($w/a = 0.2$) is required to establish a high susceptance suitable for narrow-band filters. In the second configuration, the fins provide heavy loading to the waveguide and a higher susceptance can be obtained with a moderately narrow strip ($w/a = 0.1$). Heavy fin loading not only provides a larger susceptance but one whose magnitude is less dependent upon frequency. Consequently, inductors in heavily loaded fin-line should prove to be of great value and deserve further study.

CONCLUSIONS

The application of standard microstrip techniques at millimeter wavelengths can result in problems which include excessive radiation loss, spurious coupling, dispersion, and higher mode propagation. These problems can be controlled by choosing progressively thinner substrates as the operating frequency is raised but this only serves to degrade the Q, increase tolerance problems, restrict the range over which Z_0 can be varied, and complicate the design of transitions to waveguide instrumentation. Integrated fin-line is superior to microstrip at millimeter wavelengths as the former provides eased production tolerances, compatibility with chip and beam-lead devices throughout the millimeter spectrum, and single-mode octave bandwidths, combined with the ability to construct simple transitions to waveguide. Fin-line avoids excessive miniaturization and offers low loss combined with the potential for low-cost production through batch-processing techniques.

The basic characteristics of integrated fin-line have been reviewed previously. It has been demonstrated that practical fin-line structures can provide an unloaded Q of 260–850 and that the guide wavelength can be accurately predicted by a simple equation.

Examples of solid-state and passive components have been presented which serve to illustrate the potential of integrated fin-line at millimeter wavelengths. These examples have included a p-i-n attenuator which has demonstrated the capability of constructing low-loss semiconductor mounts in fin-line. An analysis has shown that existing beam-lead devices in a simple fin-line mount can be useful well beyond 100 GHz.

Based upon the analysis and examples presented, it is clear that fin-line construction techniques can be applied to a broad class of millimeter components including mixers, oscillators, amplifiers, and phase shifters. Fin-line is also suited to the fabrication of E-plane Y junctions and is therefore compatible with three-port networks such as parametric amplifiers, phase modulators, and switching matrices.

Since integrated fin-line can provide high performance combined with low-cost batch processing, it is ideally suited to a wide range of millimeter applications including communication systems, high-resolution imaging, collision-avoidance radars, and environmental monitoring equipment.

TABLE III

SUSCEPTANCE OF FIN-LINE INDUCTORS

Frequency (GHz)	λ_0/a	Normalized Susceptance (B/Y_0) No Fin Loading $d/b = 1.0$ $w/a = 0.2$	Normalized Susceptance (B/Y_0) Heavy Fin Loading $d/b = 0.1$ $w/a = 0.1$
26.5	1.59	13.2	18.1
33.0	1.28	6.8	14.7
40.0	1.05	4.9	12.0

ACKNOWLEDGMENT

This program was sponsored by AIL under the direction of K. S. Packard, M. T. Lebenbaum, and J. J. Whelehan. D. Fleri and J. J. Taub formulated the initial program plan and made technical contributions throughout the program. Technical assistance was provided by R. Chew, R. Gibbs, L. Hernandez, A. Kunze, and W. Reinheimer.

REFERENCES

[1] D. Dobramysl, "Integrated mixer for 18 and 26 GHz," in *IEEE 1971 G-MTT Symp. Digest* (Washington, D. C.), May 16–19, 1971, pp. 18–19.

[2] T. H. Oxley, K. J. Ming, G. H. Swallow, B. J. Climer, and M. J. Sisson, "Hybrid microwave integrated circuits for millimeter wavelengths," in *IEEE 1972 G-MTT Symp. Digest* (Arlington Heights, Ill.), May 22–24, 1972, pp. 224–226.

[3] J. J. Taub, "The status of quasi-optical waveguide components for millimeter and submillimeter wavelengths," *Microwave J.*, pp. 57–62, Nov. 1970.
[4] P. J. Meier, "Two new integrated-circuit media with special advantages at millimeter wavelengths," in *IEEE 1972 G-MTT Symp. Digest* (Arlington Heights, Ill.), May 22–24, 1972, pp. 221–223.
[5] ——, "Equivalent relative permittivity and unloaded Q factor of integrated fin-line," *Electron. Lett.*, vol. 9, pp. 162–163, Apr. 1973.
[6] ——, "Microwave transmission line," U. S. Patent 3 825 863, July 1974.
[7] S. B. Cohn, "Properties of ridge wave guide," *Proc. IRE*, vol. 35, pp. 783–788, Aug. 1947.
[8] S. Hopfer, "The design of ridged waveguides," *IRE Trans. Microwave Theory Tech.*, vol. MTT-3, pp. 20–29, Oct. 1955.
[9] F. E. Gardiol, "Higher-order modes in dielectrically loaded rectangular waveguides," *IEEE Trans. Microwave Theory Tech.*, vol. MTT-16, pp. 919–924, Nov. 1968.
[10] P. H. Vartanian, W. P. Ayres, and A. L. Helgesson, "Propagation in dielectric slab loaded rectangular waveguide," *IRE Trans. Microwave Theory Tech.*, vol. MTT-6, pp. 215–222, Apr. 1958.
[11] D. Fleri, "AIL project R035 status report," Internal Memo, Oct. 1973.
[12] R. A. Pucel, D. J. Massé, and C. P. Hartwig, "Losses in mircostrip," *IEEE Trans. Microwave Theory Tech.*, vol. MTT-16, pp. 342–350, June 1968.
[13] G. C. Southworth, *Principles and Applications of Waveguide Transmission*. Princeton, N. J.: Van Nostrand, 1950, pp. 104–105.
[14] D. A. Fleri *et al.*, "A low cost X-band MIC paramp," presented at the IEEE Int. Microwave Symp., Atlanta, Ga., June 1974.
[15] Y. Konishi, K. Uenakada, N. Yazawa, N. Hoshino, and T. Takahashi, "Simplified 12-GHz low-noise converter with mounted planar circuit in waveguide," *IEEE Trans. Microwave Theory Tech.* (Short Paper), vol. MTT-22, pp. 451–454, Apr. 1974.
[16] J. J. Taub, "Design of minimum loss band-pass filters," *Microwave J.*, Nov. 1963.

Broad-Band Directional Couplers Using Microstrip with Dielectric Overlays

BORIS SHELEG, MEMBER, IEEE, AND BARRY E. SPIELMAN, MEMBER, IEEE

Abstract—**This paper presents the development of two microwave integrated circuit (MIC) broad-band, high-performance directional couplers with dielectric overlays. The respective nominal coupling values of these components are 6 and 10 dB with useful bandwidths in excess of 3.4:1. Thorough descriptions of the design procedure, performance, and fabrication techniques are presented in sufficient detail to permit duplication of these couplers. The computer-aided design method used to develop these couplers is modeled to treat parallel-coupled microstrip lines with a dielectric overlay and is also suitable for developing directional filters and Schiffman phase shifters of similar construction. This and other design methods available for developing dielectric-overlay couplers are reviewed with particular attention given to related technological areas that warrant further investigation.**

I. INTRODUCTION

THERE HAS BEEN considerable interest in developing broad-band directional couplers in a format suitable for integrated systems. The successful development of such couplers has been hampered by directivity degradation attributable to a difference between the even- and odd-mode phase velocities [1]. It has been demonstrated that the use of proper dielectric overlays on microstrip couplers offers significant relief for this directivity degradation problem [2]–[8].

Manuscript received May 17, 1974; revised August 23, 1974.
The authors are with the Microwave Techniques Branch, Electronics Division, Naval Research Laboratory, Washington, D. C. 20375.

Heretofore, components employing edge-coupled microstrip with dielectric overlays have been designed by approaches relying upon empirical modifications of data for coupled microstrip *without* overlays [2], [5], [6].

This paper describes two dielectric-overlay couplers designed by an approach which was formulated specifically for couplers using edge-coupled microstrip with a dielectric overlay. This approach has the inherent advantange of utilizing a computer-aided method of moment analysis [9] which determines the electrical characteristics of coupled microstrip *with* a dielectric overlay. The development descriptions of these couplers (6 and 10 dB) are complete, including details of hardware design and computational considerations as well as performance measurements. Following the characterization of these couplers, the salient features of the design approach here and those used previously are discussed.

II. COUPLER DEVELOPMENT

A. Design Approach and Performance

The 6- and 10-dB directional couplers to be described have two asymmetric cascaded quarter-wavelength sections (at midband) of edge-coupled microstrip lines with dielectric overlays; however, the design approach is equally applicable to symmetric couplers. Lossless coupling values for the tight and loose sections were obtained from